

SUPPLEMENTARY INFORMATION

MONITORING TRENDS IN BURN SEVERITY (MTBS)

MTBS provides a Landsat-based fire burned area dataset available for the United States (US) from 1984 to 2021 ([27,53], <https://www.mtbs.gov/>, last access January 2024). MTBS uses all Landsat 30 m measurements (version 4, 5, 7, 8, and 9) since 1984. Since mid-2015 and 2017, measurements of Sentinel 2-A and Sentinel 2-B, respectively, have been added to complement Landsat at the occasions Landsat data are not available. It is currently the largest and most comprehensive (spatially and temporally) documented fire monitoring program conducted by the US Department of Agriculture Forest Service and the US Geological Survey. MTBS uses state and federal agencies/organizations reporting systems to identify and retrieve detailed information of different fire types. The MTBS program uses these reporting systems to support all phases of the fire mapping process, such as linking fire information with burn area data. Fire agencies use prescribed fires for management of natural landscapes to reduce vegetation density and consequently fuel loads, thereby reducing wildfires risk, while private landowners often use this practice to clear land of agricultural and wildland residues, without considering it a fire risk management strategy. To avoid confusion, MTBS protocol excludes fires on agricultural land. Of the total of 26726 reported events (see Figure S1), we used 12292 classified as wildfires (ignited unintentionally), and 7923 classified as prescribed fires for the regions of interest in this study. The remaining fires classified as unknown (6300 incidents) and wildland fire use (211 incidents) were not considered. Wildland fire use represents wildfire events ignited naturally but managed afterward for ecological purposes. However, this classification is no longer used after 2009. While burned area with MTBS records can be observed for all regions and all years, the type of fires (prescribed versus wildfire) can only be determined through reporting systems. If fire events are not reported from the original reporting agency, this results in an unknown fire classification in the MTBS dataset. This could explain why for some eastern regions some years only have unknown fires identified, with few prescribed fires classified before 2000 (Figure S2).

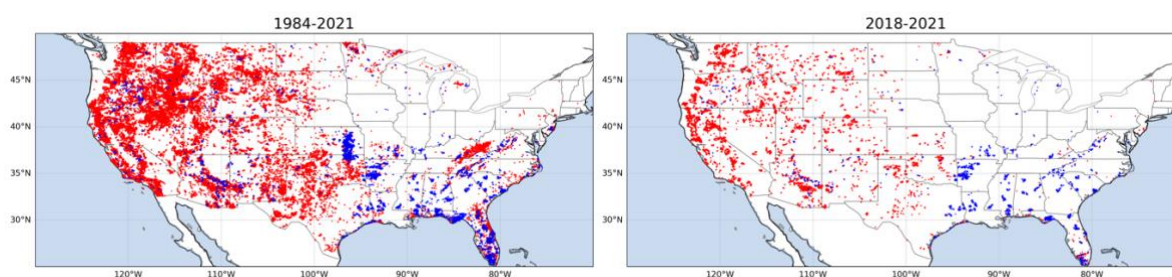


Figure S1. Distribution of prescribed fires (in blue) and wildfires (in red) over the period 1984-2021 (left panel) and the period 2018-2021 (right panel) for CONUS from the MTBS dataset. It highlights distinct spatial patterns, with wildfires predominantly concentrated in the western regions, while prescribed burning is more prevalent in the eastern regions.

Each MTBS fire consists of a fire perimeter polygon. The MTBS dataset only provides large fire events defined as burn scars $\geq 2 \text{ km}^2$ (500 acres in size) in the eastern US and $\geq 4 \text{ km}^2$ (1000 acres in size) in the western US. The states were grouped into five larger geographical regions based on the US Census Divisions with the exception of Atlantic (ATL) and East South Central (ESC) which have been grouped to include states with similar prescribed burning practices (Fig. 1b of main text). The MTBS record shows the annual wildfire burned area have been increasing from 1984 through 2021, although for PAC the increasing trend only sets off after 1998 (Fig. S2a). A reduction in prescribed fire is observed after 2012, possibly from concerns over an escaped prescribed fire in Colorado [7] that burned many houses and led to at least two fatalities. We also note two major wildfire events for WC in 2006 and 2011 were caused by severe droughts in Texas and Oklahoma (Fig. S2a and Fig. S3).

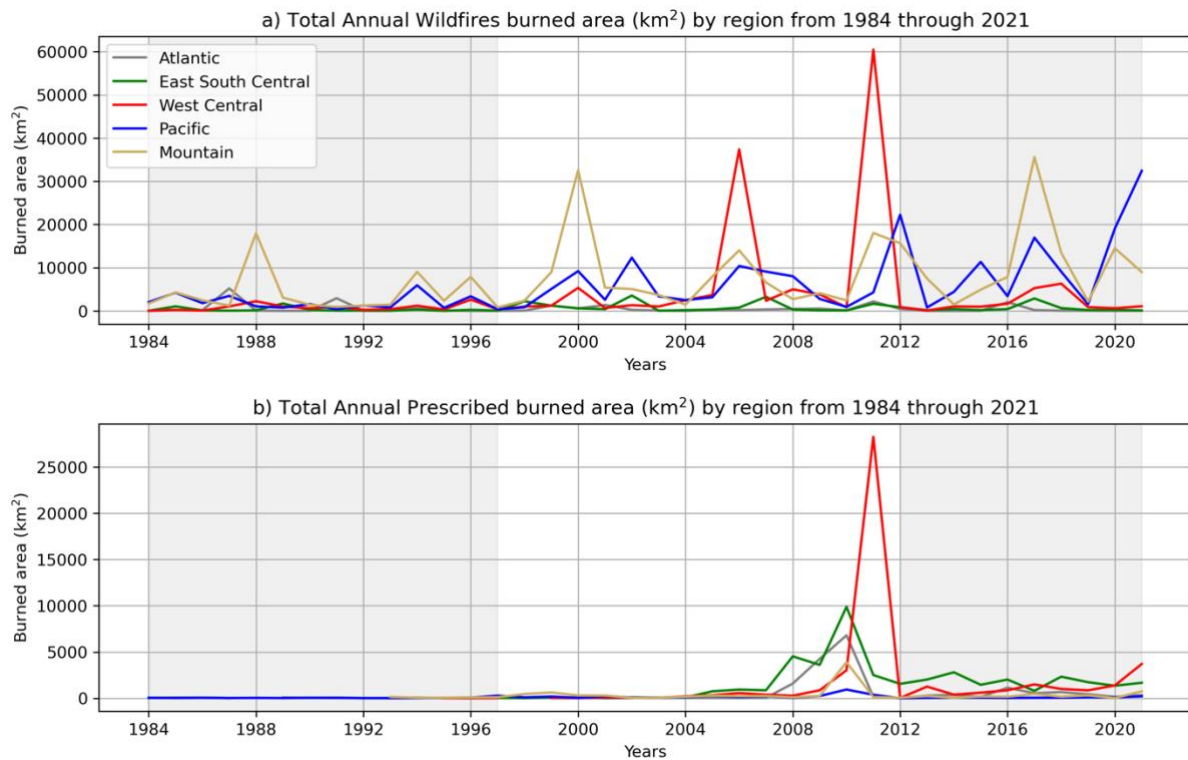


Figure S2. Overview MTBS record of prescribed fire and wildfire burned area. Time series depict annual burned area from MTBS (in km^2) of wildfires (a) and prescribed fires (b) for each of the five regions of interest. Three periods (gray/white) are highlighted: 1984-1997, 1998-2011, 2012-2021.

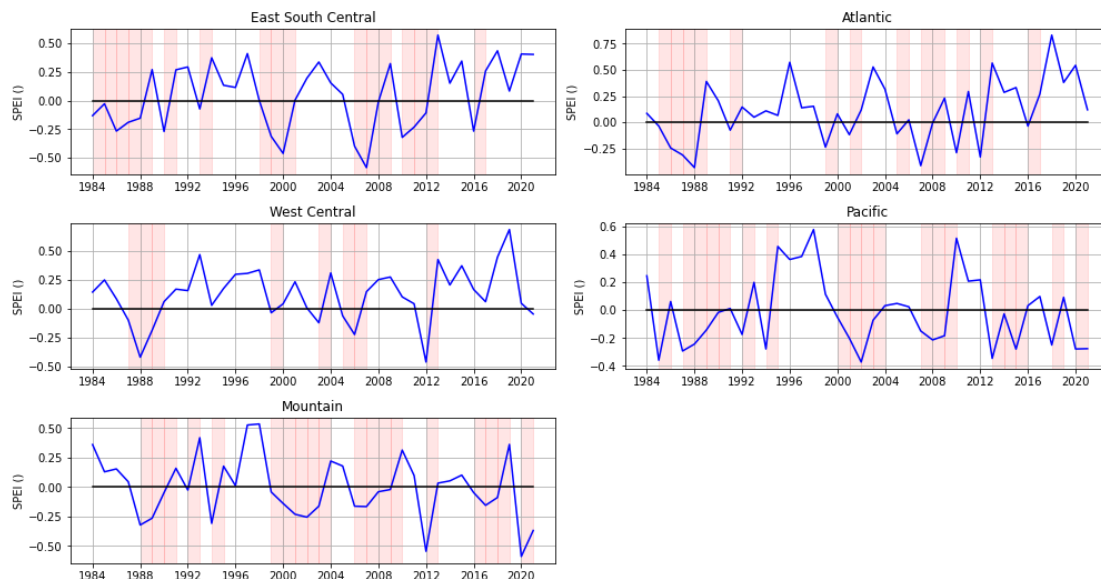


Figure S3. Regional Standardized Precipitation Evapotranspiration Index (SPEI [54]) over the period 1984-2021. This drought index uses both precipitation and temperature records to identify the accumulated deficit or surplus of the water balance, i.e., the difference between precipitation and potential evapotranspiration. Potential evapotranspiration is calculated empirically from air temperature [55]. A 1-month temporal resolution of SPEI is used for our analysis. SPEI index is used as a proxy to detect, monitor, and analyze droughts, and has the advantage to identify differences in severity and duration of drought events. Red shading represents month of negative SPEI. The two recent minimum values of SPEI for WC happened in 2006 and 2012, corresponding to two major droughts in Texas and Oklahoma (as observed with Figure S2a) with a drought in PAC from 2012-2015.

MTBS does not account for small fires typically included in land managers' reports, leading to a potential underestimation of burned area from prescribed fires in the MTBS dataset. However, when comparing MTBS total burned area for CONUS with the FireCCI51 product [51] based on the commonly used Moderate Resolution Imaging Spectroradiometer (MODIS) 500 m burned area product (MCD64A1C6, Giglio et al., 2018), MTBS consistently reports higher burned area than MODIS (Fig. S4 and Table S1).

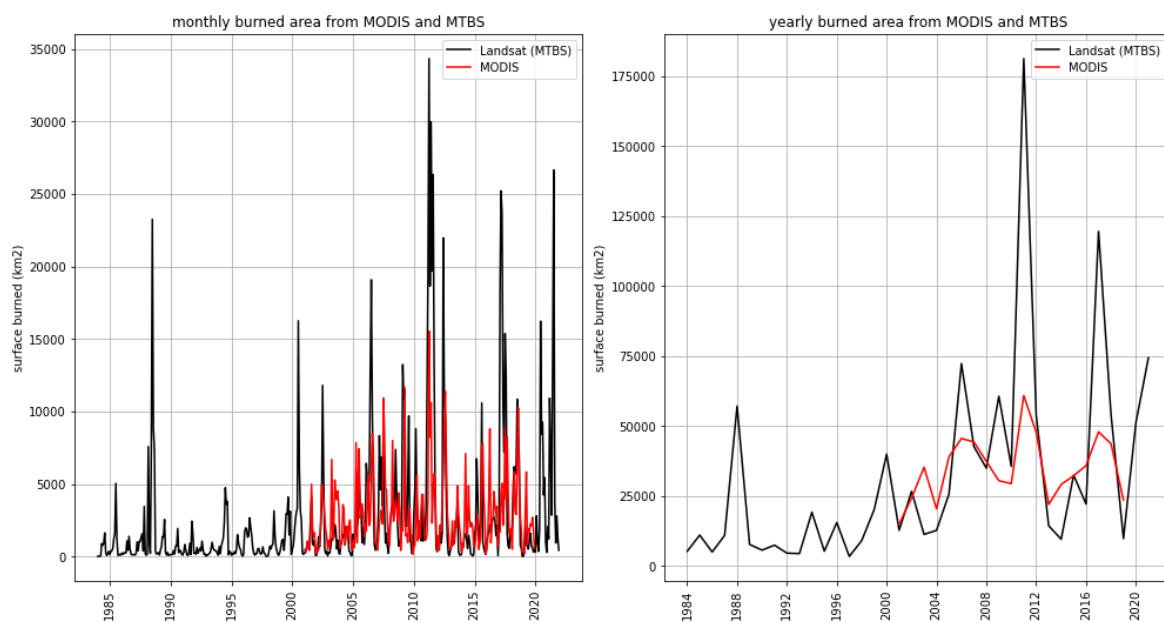


Figure S4. Comparison between burned area (in km²) from FireCCI51 (a version of MODIS burned area within the Fire_cci project from ESA, in red [51]) and the MTBS dataset (primarily based on Landsat measurements, in black) at monthly (left side) and annual time steps (right side). FireCCI51 data is limited to the period 2001-2019.

Table S1. Annual burned area (in km²) of FireCCI51 (MODIS) and MTBS (Landsat), and their differences (MODIS-MTBS), for the period 1984-2021. Average and total burned area for the period 2001-2019 are displayed in the two last rows.

Years	MODIS	MTBS	MODIS -MTBS
1984		5 171.8	
1985		10 947.5	
1986		4 895.5	
1987		10 838.2	
1988		57 052.4	
1989		7 605.3	
1990		5 573.8	
1991		7 348.7	
1992		4 489.9	
1993		4 344.0	
1994		19 118.7	
1995		5 187.3	
1996		15 437.0	
1997		3 319.6	
1998		8 989.8	
1999		20 086.8	
2000		39 866.5	
2001	14 915.1	12 683.7	2 231.5
2002	24 207.4	26 589.5	-2 382.0
2003	35 210.5	11 193.4	24 017.1
2004	20 346.8	12 635.0	7 711.8
2005	38 950.9	25 682.4	13 268.5
2006	45 503.9	72 299.1	-26 795.2
2007	44 257.8	42 589.1	1 668.7
2008	37 277.1	34 887.6	2 389.5
2009	30 409.6	60 619.8	-30 210.2
2010	29 337.8	35 524.1	-6 186.4
2011	60 846.3	181 353.8	-120 507.5
2012	47 748.7	53 769.3	-6 020.7
2013	21 899.2	14 280.0	7 619.2
2014	29 057.5	9 451.8	19 605.7
2015	32 152.8	32 385.9	-233.2
2016	35 776.5	22 068.4	13 708.0
2017	47 846.0	119 530.0	-71 684.0
2018	43 633.6	54 073.6	-10 440.0
2019	23 515.5	9 699.4	13 816.1
2020		51 194.9	
2021		74 360.5	
Average score 2001-2019:	34 889.1	43 753.5	-8 864.4
Total score 2001-2019:	662 893.0	831 316.1	-168 423.1

For our study, the surface area of each single daily fire perimeter polygon was used and aggregated to a monthly grid of 0.25°x0.25° resolution to facilitate comparison with other datasets as shown in all figures except Figures 2 and 3 in the main text. Specifically for

Figure 2, we retained the fire perimeter polygons to visualize and estimate the percentage of encroachment of wildfires on prescribed fire perimeters. Over a nearly 40-year period, there were only 8 instances of prescribed fires in proximity to wildfires starting the same days or shortly after, and these were excluded for this study (Table S2). We did not consider these potential cases of wildfires and prescribed burning as not enough information were provided to explain their proximity. While prescribed fires reduce fuel load (vegetation), wildfires might eliminate it more thoroughly, and very likely also act as a barrier for future wildfires. We did not account for this effect in our statistics of Figure 2.

Table S2. Information from the MTBS record for the period 1984-2021 on instances where prescribed fires and wildfires occurred in proximity, either on the same day or within a 4-day window. Red boxes in the drought index column highlight events that took place under drier than normal conditions.

State	Starting Day		BA (acres)		Name		Coordinate	Drought index
	Pres	Wild	Pres	Wild	Pres	Wild		
TEXAS	2005,9,17	2005,9,17	14.5	18.2	WF 10-11	WF UNIT 11 2005	29.7N-94.1W	0.09
TEXAS	2009,2,28	2009,2,28	25.9	11.9	TXR POST IKE RX 09	SABINE PASS	29.7N-94W	-1.3
IDAHO	1999,9,7	1999,9,9	26.6	19.2	WILSON RIDGE	MALLARD LAKE	42.8N-114.1W	-0.63
FLORIDA	2011,2,16	2011,2,18	3.9	6.6	UNNAMED	UNNAMED	26.9N-81.7W	-0.63
ARKANSAS	2013,3,5	2013,3,8	35.2	4.9	WILDERNESS RX	ROCK HOLLOW	36.1N-92.5W	0.39
OKLAHOMA	2014,5,10	2014,5,13	216.0	89.5	1 OKLAHOMA RANGE	100 MILE CREEK	64.0N-146.4W	-0.42
ARKANSAS	2016,2,6	2016,2,9	20.7	15.5	UNNAMED	BIG POINT	35.8N-93W	1.9
FLORIDA	2008,3,13	2008,3,17	3.6	7.9	UNNAMED	UNNAMED	2.5N-81.3W	-1.1

PREScribed FIRE AND WILDFIRE RELATIONSHIP

To determine the impact of prescribed fires on wildfires, we only considered prescribed fires occurring before wildfires. For each grid cell, we averaged 12-months of prescribed burned area recorded within a 12-month running window and the successive monthly wildfire burned area.

Once done, some filters were applied to the grid cells:

(i) Insufficient data: grid cells with fewer than 4-months of prescribed fires or wildfires burned area over the 38 years were excluded.

(ii) No prescribed fire ($R_x=0$): if a grid cell had no recorded monthly prescribed burned area but at least 4 months of wildfire burned area, this grid cell was categorized as “no Prescribed” ($R_x=0$) to assess the impact on wildfires under the absence of prescribed fires.

(iii) Only prescribed fire ($R_x>0$): if a grid cell had no recorded wildfire burned area but at least 4 months of prescribed burned area, it was included. These grid cells provide insights into wildfire suppression due to frequent and successful prescribed burns and were categorized as $R_x>0$.

(iv) Both prescribed and wildfires ($R_x>0$): if both prescribed and wildfire burned areas were recorded in a grid cell, at least a period of 13 months had to be considered. A

12-month running window with prescribed burning and successively 1 month of wildfire activity. For these grid cells, the Spearman's rank correlation coefficient was calculated, and only those with a p-value below 5% were considered. These grid cells were also considered as $R_x > 0$, to account for all prescribed fires impact on air quality.

Examples of the relation between prescribed fires and wildfires burned area inside a grid cell containing both monthly prescribed and wildfires burned area are shown in Fig S5.

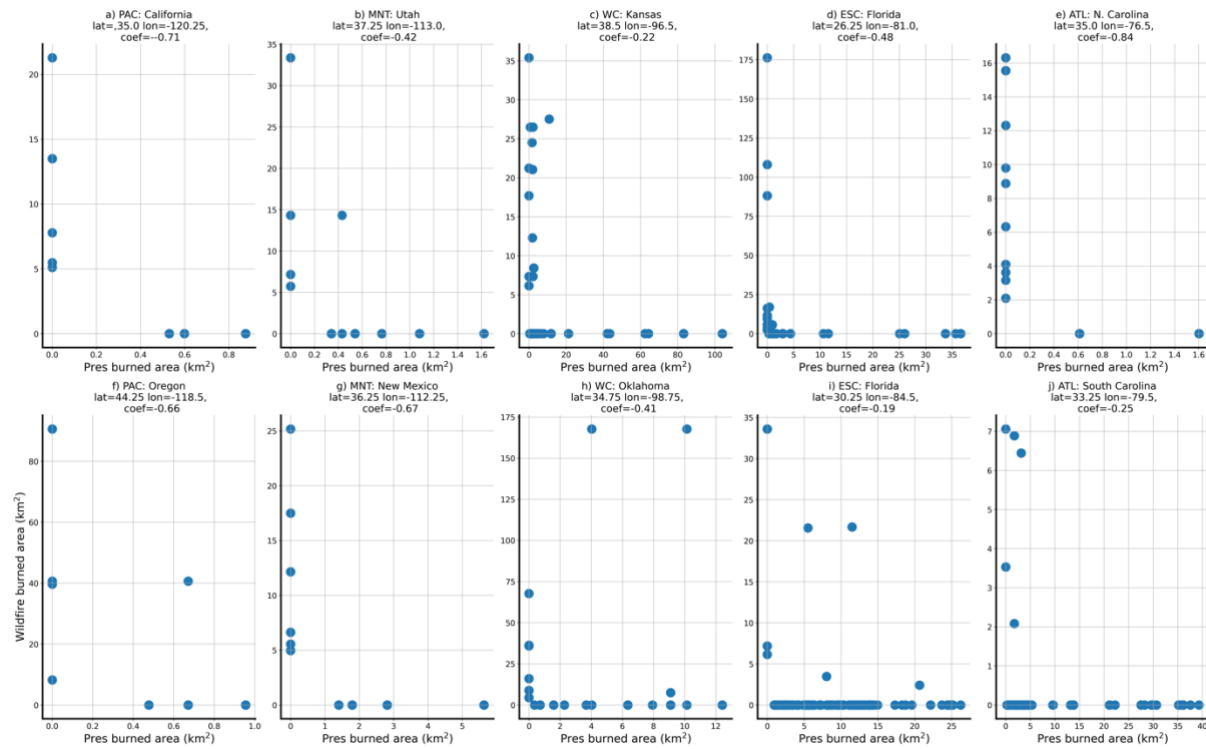


Figure S5. Examples of $0.25^\circ \times 0.25^\circ$ grid cells -similar to Fig. 1c-g-, showing the relation between the running 12-month average of prescribed burned area and the successive monthly wildfire burned area for two grid cells per region.

CARBON MONOXIDE (CO) CONCENTRATIONS

For the air quality aspect of this study, we used measurements of carbon monoxide (CO) column densities from the TROPOspheric Monitoring Instrument (TROPOMI [36]), launched in October 2017. The CO column densities were obtained using the Shortwave Infrared Carbon Monoxide Retrieval algorithm (SICOR [37,38]). TROPOMI provides daily global coverage with spatial resolution of $7 \times 5.5 \text{ km}^2$ at nadir and with a $\sim 2600 \text{ km}$ swath. We filtered the data, using a data quality assurance value threshold of ≥ 0.5 , to include clear sky, clear-sky-like, and cloudy sky conditions with cloud tops under 5000m elevation [39]. Previous studies have validated the CO retrievals against ground-based measurements from the TCCON network [40]. For clear-sky-like conditions, mean biases and standard deviation have been reported to be 6.2 ppb and 3.9 ppb, respectively [40]. We used a super-observation approach following the method of [41] to generate representative data at a coarser horizontal resolution of $0.25^\circ \times 0.25^\circ$ to account for all information at the fire source, the plume, and surrounding areas. The observations are aggregated and averaged to a grid using their grid area overlap providing weights for the

aggregation. This approach and the coarse horizontal resolution dilute the signal at the fire source, but it ensures minimal information loss around fire hotspots. In addition, this approach is mass conserving, meaning that the grid cell average CO has a lower average measurement error when there is high data coverage.

AIR QUALITY ANALYSIS METHODOLOGY

Our objective is to assess the impact of wildfires and prescribed fires on air quality for our 38-year study-period, using TROPOMI CO (during 2018-2021) as proxy. Specifically, we want to quantify to what extent air quality is degraded when no prescribed burning is performed ($R_x=0$ thus only wildfires), or when there is prescribed burning performed ($R_x>0$) at a regional scale. We took CO super-observations at each specific fire location to derive daily CO column densities from both prescribed fires and wildfires. Local enhancements were determined by subtracting background column densities determined 30km upwind from the fire sources using 10m wind direction data from ECMWF ERA-5 reanalysis data [57] at the corresponding local time. When the burned area was distributed over multiple super-observations, we considered all relevant grid cells. If the background extended into a grid cell containing a fire (for example, if the burned area covered two grid cells), we determined the background upwind to the next adjacent grid cell without a fire. For each day and at each fire denoted by i , we use the $0.25^\circ \times 0.25^\circ$ grid-cell area (A in m^2) and CO enhancement (in mol/m^2) to calculate proxy of CO mass in kg for each grid-cell i , as follows:

$$TROP O_{Wild,day,i} = (CO_{Wild,i} - CO_{i,bck}) \cdot A \cdot M \quad (4)$$

$$TROP O_{Rx,day,i} = (CO_{Rx,i} - CO_{i,bck}) \cdot A \cdot M \quad (5)$$

Where M is the molecular weight of CO (0.028 kg/mol), and bck denotes the background CO level upwind from the fire.

$$TROP O_{Wild,month,j} = \sum_{day} \sum_i [TROP O_{Wild,day,i}] \quad (6)$$

$$TROP O_{Rx,month,j} = \sum_{day} \sum_i [TROP O_{Rx,day,i}] \quad (7)$$

We take the sum of all daily values over each region, denoted by j , to obtain proxy corresponding to the monthly and regional amount of CO.

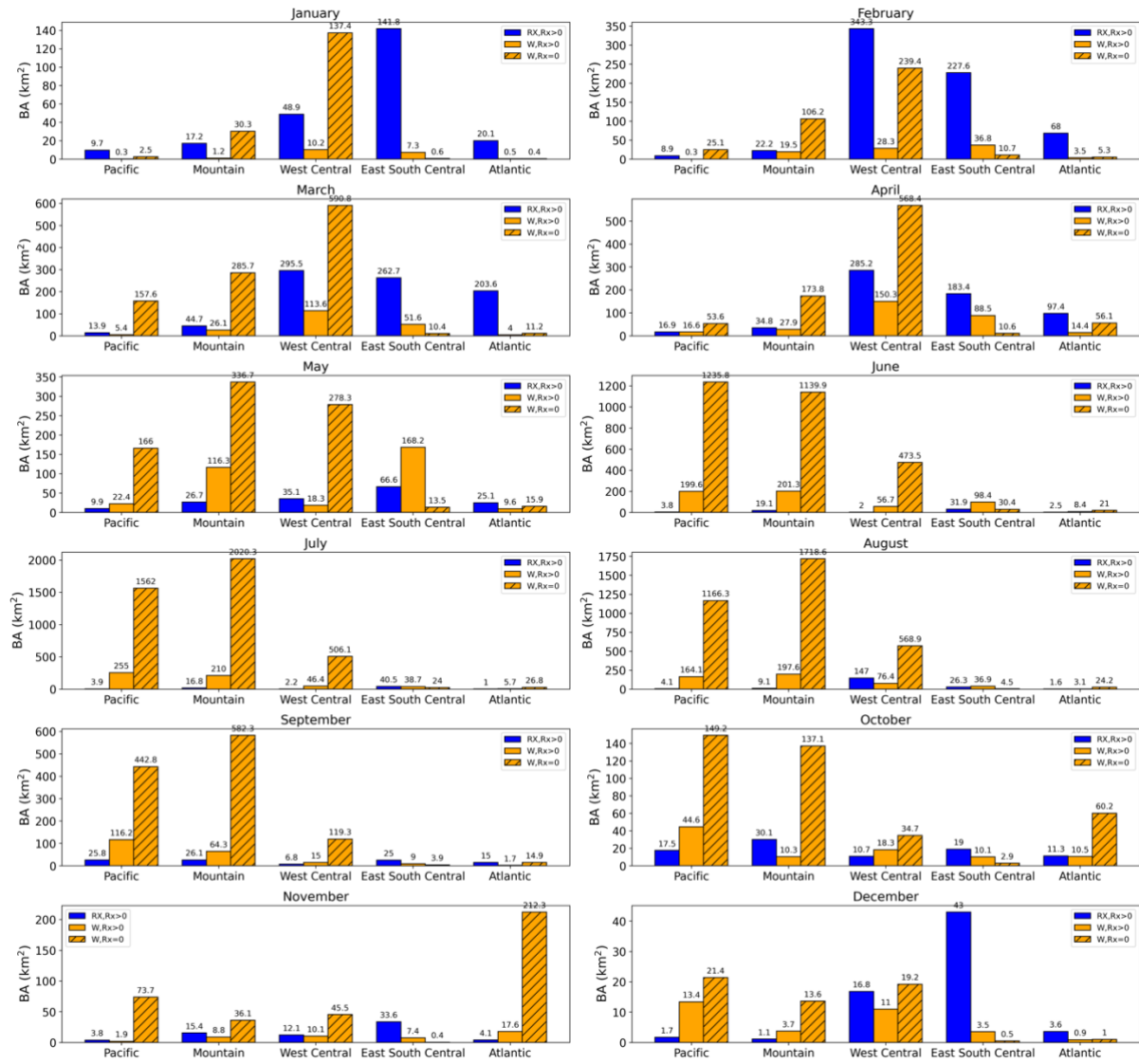


Figure S6. Monthly regional burned area (in km²) averaged over the period 1984-2021 of prescribed fires (in blue) and wildfires (in orange) for the two regimes Rx=0 (hatched bar) and Rx>0 (plain bars). Corresponding values are labelled above each bar. Panels from left to right and top to bottom correspond to a specific month from January to December. Inside each panel, from left to right are displayed the regions PAC, MNT, WC, ESC, and ATL. Monthly results per region were derived by first using the monthly mean of burned area for each grid cell (depending on specific regime of prescribed fires) and then calculating the sum of all grid cells per region.

We derive three different estimates of CO pollution by using the calculated regional and monthly proxy of TROPOMI CO mass during 2018-2021 (calculated using equations 4-7) and scaled with 38-year average monthly wildfire burned area data (using equations 8-10 shown here below): (1) wildfire air pollution when no prescribed burning is performed (calculated with equation 8), (2) prescribed burning air pollution for areas where prescribed burning is performed (Rx>0, calculated with equation 9), and (3) wildfire air pollution for areas where prescribed burning is performed (Rx>0, calculated with equation 10).

See below the three main equations indicative of CO air pollution under the two different prescribed burning regimes:

$$CO_{Wild,Rx=0} = \sum_{month=1}^{48} \frac{TROPO_{Wild,month,j}}{BA_{Wild,month,j}} \cdot BA38_{Wild,Rx=0,m,j} \quad (8)$$

$$CO_{Rx,Rx>0} = \sum_{month=1}^{48} \frac{TROPO_{Rx,month,j}}{BA_{Rx,month,j}} \cdot BA38_{Rx,Rx>0,m,j} \quad (9)$$

$$CO_{Wild,Rx>0} = \sum_{month=1}^{48} \frac{TROPO_{Wild,month,j}}{BA_{Wild,month,j}} \cdot BA38_{Wild,Rx>0,m,j} \quad (10)$$

where $BA38_{Wild,Rx=0,m,j}$ denotes the monthly (from January to December) mean wildfire burned area of the period 1984-2021 from all regional grid cells where no prescribed fires were performed but wildfires occurred; $BA38_{Rx,Rx>0,m,j}$ denotes the regional monthly mean prescribed burned area over the same period, considering areas where prescribed burning occurred ($Rx>0$); and $BA38_{Wild,Rx>0,m,j}$ the corresponding wildfire burned area when considering areas where prescribed burning occurred ($Rx>0$). The index m corresponds to the 38-year average value for each month from January to December. The values for $BA38_{Wild,Rx=0,m,j}$, $BA38_{Rx,Rx>0,m,j}$ and $BA38_{Wild,Rx>0,m,j}$ are from Figure S6. Table S3 gives the regional and annual mean of burned area (sum over the 12 months from the 38-year average) for prescribed fires and wildfires depending on the 2 regimes ($Rx>0$ and $Rx=0$). $BA_{Wild,month,j}$ and $BA_{Rx,month,j}$ denote the actual 48 monthly burned area values during 2018 – 2021 (denoted with *month*) for each region. Regional estimates are denoted with j index.

Table S3. Annual average regional burned area (in km²) from the period 1984 – 2021 of wildfires and prescribed fires for each region based on two prescribed fire regimes: $Rx=0$ and $Rx>0$. Values are estimated from the results of Figure S6. The final column shows the annual mean and regional total burned area (wildfires + prescribed fires). For each region, the smaller total burned area based on the two regimes is highlighted in green, while the larger total burned area is highlighted in red.

		38 years of burned area (in km ²)		
		Pres	Wild	Pres + Wild
West Central	Rx = 0	0	3 581.4	3 581.4
	Rx > 0	1205.5	554.6	1 760.2
East South Central	Rx = 0	0	112.4	112.4
	Rx > 0	1 101.4	556.2	1 657.6
Atlantic	Rx = 0	0	449.4	449.4
	Rx > 0	453.3	79.9	533.2
Pacific	Rx = 0	0	5 055.9	5 055.9
	Rx > 0	120.1	839.7	959.7
Mountain	Rx = 0	0	6 580.7	6 580.7
	Rx > 0	263.5	886.9	1 150.4

Figure 4, of the main text, represents the total air pollution proxy for each region depending on the two prescribed regimes rescaled from the 38-year period. For each region, the air pollution in the $Rx=0$ fire regime is shown by colored triangles (estimated

from equation 8) and the impact of having prescribed burning ($R_x > 0$) is shown by colored stars (estimated from both equations 9 and 10). The 38-years rescaled regional CO air pollution (from both prescribed and wildfires) depending on the two regimes are displayed in Table S4.

Table S4. CO air pollution proxy (sum of prescribed and wildfires, in Gg) depending on the two prescribed fire regimes per region and rescaled for the 38-years. For ESC and ATL regions, in areas where $R_x > 0$, we see higher CO pollution than in areas where $R_x = 0$. This is because prescribed fire burned area are very dominant relative to the wildfire burned area in this region. For the western regions, however, at areas where $R_x > 0$, we do not see a degradation of air quality relative to $R_x = 0$, since the potential wildfire reduction accomplished helps significantly reduce the total CO pollution. This is particularly visible for regions where wildfires are dominant, like PAC.

	PAC	MNT	WC	ESC	ATL
$R_x = 0$	29.2	19.4	13.4	0.4	7.7
$R_x > 0$	5.5	3.6	6.4	8.4	8.0

BOTTOM-UP EMISSIONS

CO fire and anthropogenic bottom-up emissions are used in this study to highlight the fire impact in each region relative to non-fire anthropogenic CO emissions. The Global Fire Emission Database version 4 with small fires (GFED41s [42]) provides fire emissions for a large number of trace gases and aerosols at a $0.25^\circ \times 0.25^\circ$ spatial resolution. The original product used the MODIS burned area product Collection 5.1 MCD64A1 at 500m spatial resolution [43] as well as information on fuel consumption per unit area burned using the Carnegie-Ames-Stanford approach (CASA) biogeochemical model [44] at $0.25^\circ \times 0.25^\circ$ spatial resolution. It also included information of small fire burned area using a statistical approach by combining MODIS active fire product (MOD14) with burned area. Due to upgrades in the MODIS burned area product from collection 5.1 to collection 6, GFED41s emissions from 2017 onward are not based on MODIS burned area anymore, but on linear relationships between MODIS active fire detections and the 2003-2016 climatology of GFED41s emissions. The conversion from combusted dry matter to emissions of trace gases is done using the emissions factor (EF) synthesis from [45], providing averaged CO EFs for only 6 general vegetation types: deforestation, peat, agricultural, temperate forest, boreal forest, and savanna/grassland.

The anthropogenic fluxes are from the CAMS-GLOB-ANT inventory version 5 [46] at a spatial resolution of $0.1^\circ \times 0.1^\circ$. The dataset is derived from the spatial distribution and monthly emissions from Emissions Database for Global Atmospheric Research version 5 (EDGAR v5 [47]) providing data for the period 1970-2015. The emissions provided by the Community Emissions Data System (CEDS [48]) are used for extrapolation of the emissions to the most recent years. This dataset also includes updated ship and aircraft emissions. To calculate the ratio of fire emissions relative to anthropogenic emissions in Figure S7, we only used emission data for the months experiencing fires in each region of interest. We can see that the western regions have relatively more CO fire emissions than anthropogenic emissions compared to the eastern regions. Particularly, the Pacific region has CO fire emissions about half of the CO anthropogenic emissions.

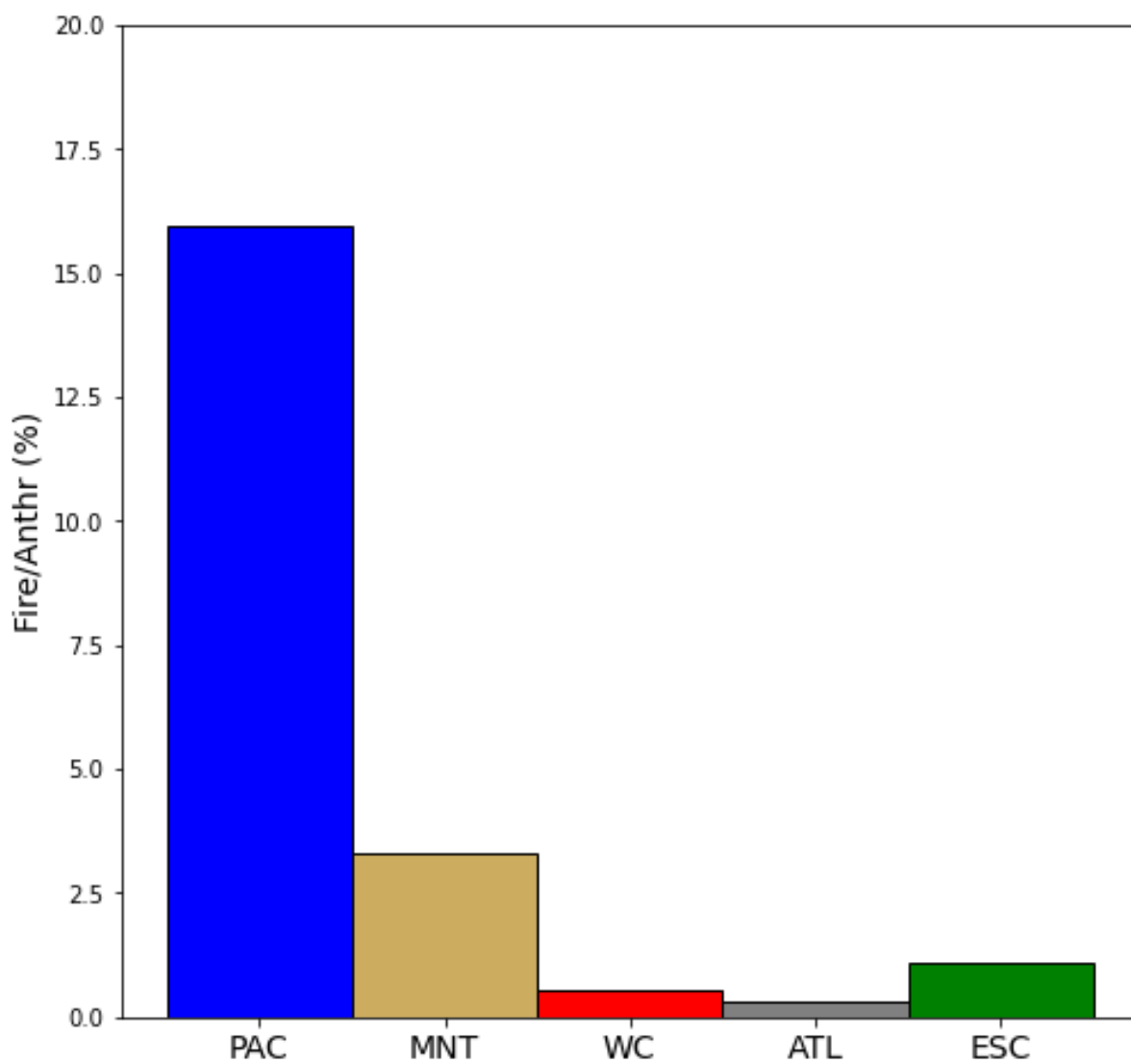


Figure S7. CO fire emissions (wildfires and prescribed fires) relative to all non-fire anthropogenic emissions (in %) for each region over the period 2018-2021.